



Comparison of fouling mechanisms in low-pressure membrane (MF/UF) filtration of secondary effluent

Shobha Muthukumaran^{a,*}, Jega V. Jegatheesan^b, Kanagaratnam Baskaran^b

^aFaculty of Health Engineering and Science, Victoria University, Melbourne, Victoria 8001, Australia

Tel. +61 3 9919 4859; Fax: +61 3 9919 4139; email: Shobha.Muthukumaran@vu.edu.au

^bFaculty of Science & Technology, Deakin University, Geelong, Victoria 3217, Australia

Received 19 March 2013; Accepted 1 April 2013

ABSTRACT

Membrane filtration in municipal wastewater treatment is being increasingly used to improve the quality of water and increase the productivity of existing plants. However, membrane fouling encountered in reclamation of municipal wastewater represents serious design and operational concern. There are several fouling models which are being developed and used as a powerful tool to increase the understanding of the fouling mechanisms and its key characteristics that influence the design of optimal process and operating conditions. This study investigates and compares the fouling mechanisms of three different types of polymeric and ceramic ultrafiltration (UF) and microfiltration (MF) membranes in the recovery of water from secondary effluent. The result demonstrated that ceramic UF membrane produced very high quality of water compared to polymeric UF and ceramic MF membranes. Out of four fouling models used to fit the experimental flux data, cake filtration and pore narrowing and complete pore blocking models predicted the initial fluxes of polymeric UF membrane more accurately. On the other hand, the cake filtration and pore narrowing models predicted the performance of ceramic UF membrane. Whereas, pore narrowing model predicted the performance of ceramic MF membrane more precisely compared to other three models. Further, the application of unified membrane fouling index (UMFI) was used to assess the fouling potential of the membranes. Good agreement between UMFI and other models was found.

Keywords: Ceramic membrane; Polymeric membrane; Microfiltration; Ultrafiltration; Secondary effluent; Fouling models; Unified membrane fouling index

1. Introduction

Membrane separation technologies such as ultrafiltration (UF) and microfiltration (MF) are the emerging

technologies that can be used for the removal of all suspended solids and a fraction of dissolved solids from wastewater. However, membrane fouling is one of the major problems encountered in the operation of membrane systems used in the treatment of

*Corresponding author.

Presented at the Fifth Annual International Conference on "Challenges in Environmental Science & Engineering—CESE 2012" Melbourne, Australia, 9–13 September 2012

wastewater. Fouling occurs through the deposition of small colloidal particles on the inner walls of the membrane's pores (standard blocking or pore narrowing), blocking the membrane pore openings (complete blocking) and build-up of particles in the form of a cake layer (cake filtration). Fouling due to blocking and cake formation is assumed to be the predominant mechanism in UF and MF filtration [1]. In general, pore blockage increases the membrane resistance, while cake formation creates an additional layer of resistance to permeate flow [2]. Reversible fouling resulting from cake formation was found to be weakly dependent on membrane surface chemistry; in contrast, irreversible fouling resulting from pore blockage showed a marked dependence on surface chemistry [3]. Membrane fouling is dependent on the various

parameters, such as operating conditions, nature of the particle and the nature of the membrane [4]. In wastewater reuse treatment, very high-molecular weight organic materials comprised of hydrophilic components, such as soluble microbial products and protein-like extracellular matter were found to be the major cause of membrane irreversible fouling [5]. Several researchers have recognised that the presence of smaller particles also causes severe fouling and leads to irreversible fouling [1,6,7]. According to Soffer et al. [7], fouling due to pore blocking was much more severe than cake layer build up and it can be significantly reduced by increasing the particle size. This result is consistent with another study by Boerlage et al. [1,8,9], who found that there is increase in the fouling index to the deposition of small particles

Table 1
Characteristics of membranes

Specification	Ceramic MF membrane	Polymeric UF membrane	Ceramic UF membrane
Manufacturer	Tami industries	Koch membrane Systems	Tami industries
Material	Zirconium/Titanium dioxide	Polyethersulfone	Zirconium/Titanium dioxide
Molecular weight cut off/pore size	1.4 μm	25 kDa	1 kDa
Membrane operating pressure	Hydrophilic <10 bar	Hydrophilic 3–14 bar	Hydrophilic <10 bar
Operating pH	0–14	0–14	0–14
Operating temperature	<350°C but change in temperature must lower than 10°C/min	70°C	<350°C but change in temperature must lower than 10°C/min
Membrane area	0.5 m ²	5.6 m ²	0.35 m ²

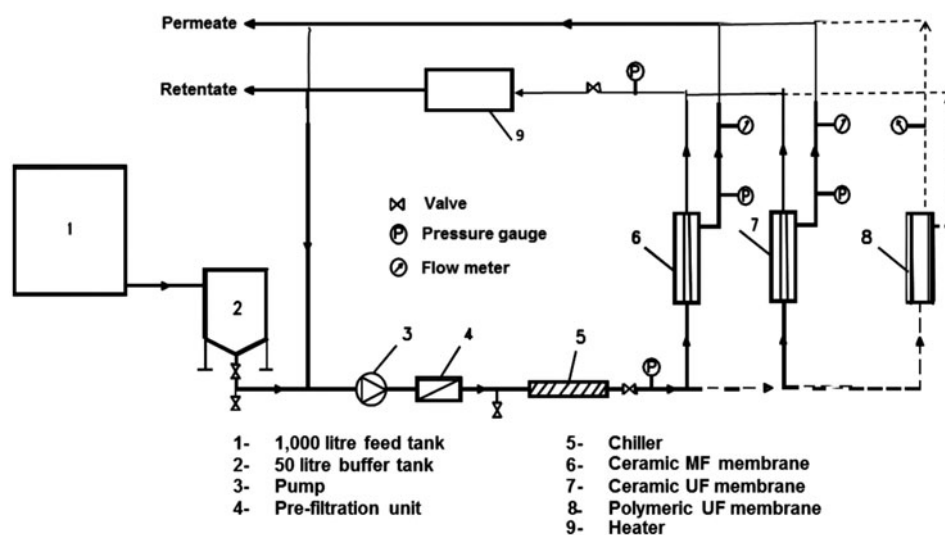


Fig. 1. Schematic diagram of experimental installation.

Table 2
The physical and chemical characteristics of the synthetic secondary wastewater

Parameter	Value
Turbidity, NTU	22.8
EC, $\mu\text{S}/\text{cm}$	340
COD, mg/l	39
Absorbance (254 nm)	0.591
Colour (filtered through filter paper 0.45 μm), ADMI	81
pH	7.73

within the pores of the membrane. As discussed by Sondhi et al. [10], for membranes where the particle size is smaller than the pore size, the fouling dynamics were expected to be dominated by pore blocking or narrowing, but fouling dynamics were most accurately represented by considering the combined effects of simultaneous pore blocking, pore narrowing and cake formation.

The problem of fouling limits membrane process efficiency leads to flux decline, permeate quality decrease, gradual ageing and eventual loss of integrity of the membranes [11,12]. This leads to a frequent cleaning and/or replacement of membranes resulting increase in operating costs. For more efficient use of membrane system in wastewater treatment, it is essential to understand more about the irreversible fouling that requires chemical cleaning. Development of effective methods to control fouling is based on understanding of the fouling mechanism and the influence of the process parameters on the membrane fouling. There are several studies on membrane applications to wastewater treatment that have been carried out to investigate and model membrane fouling [13–15]. The aim of this study is to increase the understanding of fouling mechanisms of both the ceramic and polymeric membranes using various fouling models, such as cake filtration model, pore narrowing model, combination of external and progressive internal fouling and complete pore blocking model. These models have the inherent advantage of being able to predict the process behaviour and provide valuable information for the design of filtration processes. Recently, unified membrane fouling index (UMFI) was developed to qualitatively compare membrane fouling for a given type of water, irrespective of the membrane operational conditions [16]. The specific aims of this study are to (1) evaluate the rate of fouling of membrane under the different transmembrane pressure (TMP), (2) selecting an appropriate mathematical model to predict the performance of the membranes and quantifying the corresponding

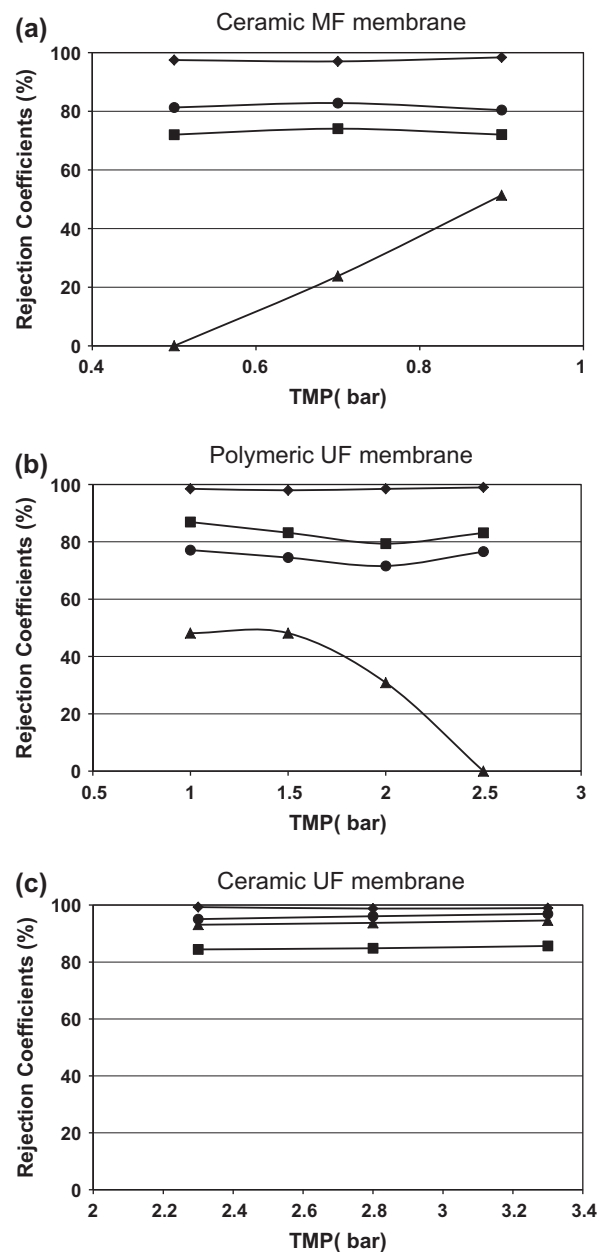


Fig. 2. Influence of TMP on the rejection coefficients: COD (●), colour (▲), absorbance 254 nm (■) and turbidity (◆).

membrane resistances and (3) applicability of UMFI to quantitatively assess the fouling potential.

2. Materials and methods

2.1. Pilot scale filtration system

The experiments were performed with UF and MF membranes. The spiral polymeric UF membrane was supplied by Koch membrane systems and tubular ceramic UF and MF membrane was supplied by Tami

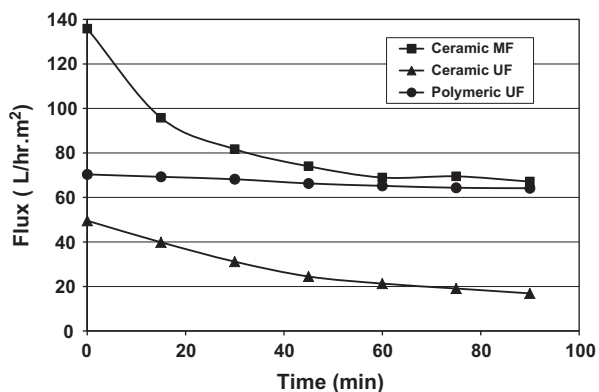


Fig. 3. Flux decay patterns of ceramic UF (TMP=2.8 bar and $T=25^{\circ}\text{C}$), ceramic MF (TMP=0.7 bar and $T=25^{\circ}\text{C}$) and polymeric UF (TMP=2 bar and $T=25^{\circ}\text{C}$) membranes as a function of time.

industries. The characteristics of these membranes are listed in Table 1.

Experiments were carried out using a pilot scale cross-flow mode filtration apparatus supplied by Liquids Technology, Australia. A diagram of the membrane pilot system is shown in Fig. 1. A synthetic secondary wastewater was prepared from a sterile concentrated solution with the composition shown in previous study [17] and used throughout this study. The synthetic secondary wastewater contains organic compounds, such as humin, tannin, lignin, protein and high molecular carbohydrates. The concentrated feed solution was stored in a refrigerator and diluted with tap water to the desired concentration before it was fed to the membrane system. The physical and chemical characteristics of the synthetic secondary

wastewater are shown in Table 2 and used throughout this study.

The experimental set-up was described in detail in a previous publication [18], and basically consists of 1,000 L container, buffer feed tank, 100 μm mesh strainer, heat exchanger/chiller unit and membrane modules. The cross-flow velocity of 0.2 m/s was used for all the experiments. The flow rates (Q_f) of permeate and retentate were measured by hydraulic flow metres installed on the system. All the filtration experiments were conducted in tangential cross-flow mode with partial retentate recycle and continuous removal of the permeate stream.

2.2. Membrane characterisation

Prior to wastewater filtration, membranes were operated with clean tap water in order to evaluate the dependence of the water flux on the TMP. The applied pressures during this process were modified according to the membrane filtration ranges; thus, the maximum TMP was 2.5 bar for the polymeric UF membrane, 3.3 bar for the ceramic UF membrane and 0.9 bar for the ceramic MF membrane. The water flux increased with increasing TMP, obtained a linear relationship with high correlation coefficients. The slope of this straight line is the pure water hydraulic permeability (L_p) which better characterises a membrane in filtration processes. The L_p values are 378 and 40 and 17 L/h m² bar for ceramic MF, polymeric UF and ceramic UF membranes, respectively at 25 $^{\circ}\text{C}$. The hydraulic permeability of the ceramic MF was very much higher than that of the UF membranes.

Table 3

Values of filtration resistances obtained in the MF and UF experiments performed

TMP bar	$R_m \times 10^{-13}$ (m^{-1})	$R_t \times 10^{-13}$ (m^{-1})	$R_f \times 10^{-13}$ (m^{-1})	$R_{ef} \times 10^{-13}$ (m^{-1})	$R_{if} \times 10^{-13}$ (m^{-1})	$R_m/R_t \times 100$ (%)	$R_f/R_t \times 100$ (%)
<i>Ceramic MF membrane (1.4 μm)</i>							
0.9	0.137	0.262	0.125	0.017	0.108	52	48
0.7	0.170	0.375	0.206	0.128	0.078	45	55
0.5	0.210	0.385	0.175	0.052	0.123	55	45
<i>Polymeric UF membrane (25 kDa)</i>							
2.5	1.008	1.043	0.035	0.011	0.024	97	3
2.0	1.008	1.122	0.114	0.015	0.099	90	10
1.5	1.008	1.093	0.085	0.019	0.065	92	8
<i>Ceramic UF membrane (1 kDa)</i>							
3.3	1.968	6.162	4.194	1.166	3.028	32	68
2.8	1.955	5.964	4.010	0.282	3.727	33	67
2.3	1.890	4.315	2.425	0.232	2.193	43	57

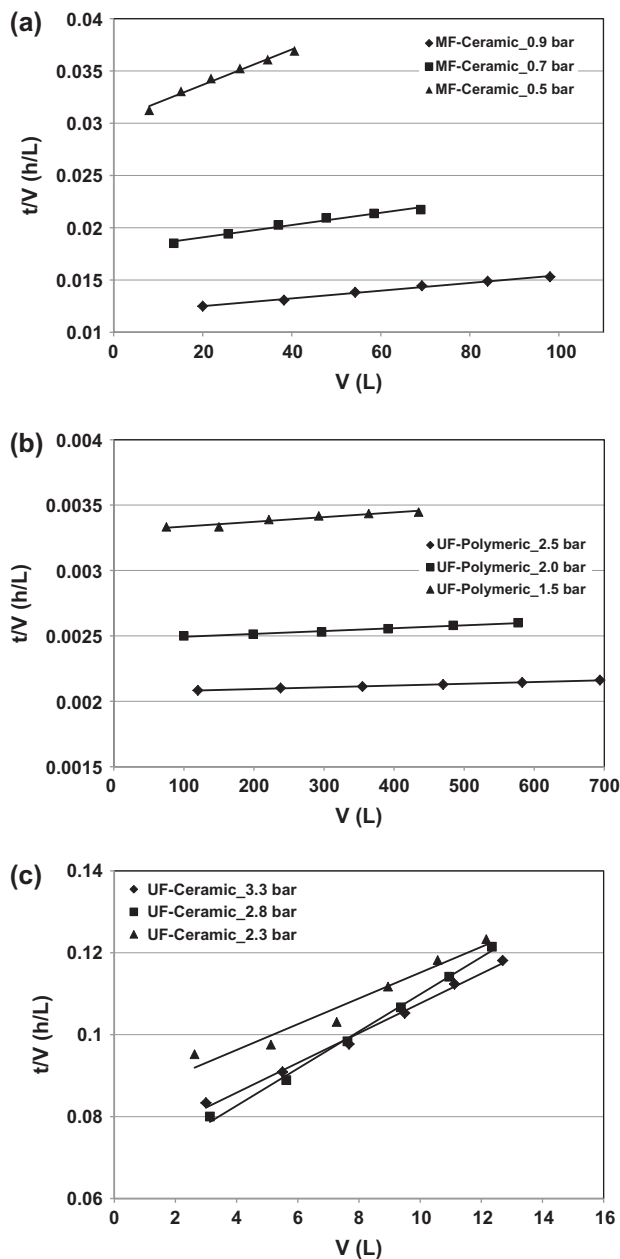


Fig. 4. Cake filtration model fitting to the experimental data obtained in (a) ceramic MF, (b) polymeric UF and (c) ceramic UF experiments (cross flow velocity = 0.2 m/s and $T = 25^\circ\text{C}$).

2.3. Analytical method

Permeate samples were collected at predetermined intervals and stored at 4°C until analysis. The parameters that measure the pollutant content of the wastewaters in both feed and permeate samples were analysed according to the procedures outlined in the standard methods [19]. All the experiments were conducted in duplicate. The chemical oxygen demand

(COD) in the samples was determined by spectroquant Nova 60 (Photometer: SQ Nova 60, Merck, Germany). Absorbance was measured as the absorbant values at 254 nm by spectroquant Photo 300 (Spectroquant Pharo 300, Merck KGaA, Germany). Colour was determined using Spectrophotometer DR/4000V (Hach company, Loveland, USA). Other parameters including: turbidity pH and electrical conductivity were analysed with 2100P (Hach company, Loveland, USA), pH 315i/SET (WTW Wissenschaftlich – Technische Werkstätten, Germany) and LF 330/SET (WTW Wissenschaftlich – Technische Werkstätten, Germany) meters, respectively.

2.4. Rejection coefficients

The effectiveness of filtration processes in the removal of organic matter present in synthetic wastewater was evaluated by rejection coefficients. The pollution indices selected in the present study were COD, absorbance at 254 nm, turbidity and colour. The rejection coefficients were determined using the following Eq. (1), for all the experiments performed.

The rejection coefficient in the case of $f_{\text{Turbidity}}$ was defined by

$$f_{\text{Turbidity}} = \frac{(\text{Turbidity})_F - (\text{Turbidity})_P}{(\text{Turbidity})_F} \times 100 \quad (1)$$

where $(\text{Turbidity})_F$ and $(\text{Turbidity})_P$ represent the turbidity on the feed and permeate streams, respectively. Similar definition equations were used for the remaining rejection coefficients.

3. Results and discussion

3.1. Treatability of the wastewater

The rejection coefficients were determined using Eq. (1) as shown in Fig. 2. In the case of ceramic MF membrane, there was a very high removal of turbidity (>95%) and high removal of COD (>80%) and moderate removal of absorbance (>75%) under all TMP studied, and the colour removal increases from 0 to 50% when the TMP was increased. Whereas, for polymeric UF membrane there was a very high removal of turbidity (>95%) and high removal of absorbance (>80%) and moderate removal of COD (>75%) under all TMP studied, and the colour removal decreases from 50 to 0% when the TMP was increased. On the other hand, with ceramic UF membrane there was very high removal of turbidity (>95%), COD (>95%) and colour (>92%) and high removal of absorbance (>85%). This result shows that there is low rejections

Table 4

Determination of parameter αC_w and correlation coefficients R^2 from the cake filtration model for the UF and MF experiments

TMP bar	Initial flux (L/h m ²)		αC_w (m ⁻²)	Error (%)	R^2
	Model	Experimental			
<i>Ceramic MF membrane (1.4 μm)</i>					
0.9	170	206	1.15E + 10	-21.177	0.994
0.7	93	110	1.33E + 10	-18.279	0.977
0.5	66	76	1.63E + 10	-15.151	0.983
<i>Polymeric UF membrane (25 kDa)</i>					
2.5	85.03	85.7	5.38E + 09	-0.783	0.996
2.0	71.43	71.4	9.03E + 09	0.04	0.985
1.5	54.11	53.5	1.37E + 10	1.132	0.934
<i>Ceramic UF membrane (1 kDa)</i>					
3.3	41	42.86	6.84E + 11	-4.529	0.995
2.8	44	42.86	9.28E + 11	2.597	0.996
2.3	34	35.71	4.93E + 11	-5.042	0.952

of pollution parameters with polymeric UF and ceramic MF membranes than ceramic UF membrane, as these membranes have bigger pore size that cannot remove pollutants smaller than their pore size. According to Lee et al. [20], most of the dissolved organic carbon in the secondary effluent has a molecular weight smaller than MWCO of 10 kDa, and without significant pre-treatment most organics in secondary effluent should pass through the UF membrane having a higher pore size of 100 kDa. In this study, both polymeric UF and ceramic MF membranes with a pore size of 25 kDa and 1.4 μ m did not completely removed foulants as majority of the organics pass through the membranes. Whereas, ceramic UF membrane with a pore size of 1 kDa did completely removed the foulants as most of the organic accumulated on the surface and pores of the membrane. These results are qualitatively supported by the rejection coefficients determination discussed above. The fouling mechanism of all the three membranes were confirmed by fitting the various fouling models which are discussed in the following section.

3.2. Comparison of ceramic and polymeric UF and MF membranes

Fig. 3 shows the comparison of experimental permeate flux for three different membranes. In general, at the start of the filtration when the membrane is clean, the particulate pollutants were rejected by the size of the membrane pores. Subsequently, particles start accumulates near the

membrane surface form a cake layer which assists in pollutant removal. However, both pore blockage and cake layer fouling mechanisms decreases the permeate flux rate which are the key factors governing the application of membrane system. In these trials, the permeate flux decline through the ceramic membranes were significantly more rapid than through the polymeric membrane. There were more than 50% permeate flux declined in both the ceramic membranes across all the TMPs studied. However, the permeate flux decline for the polymeric membrane was less than 10% across all the TMPs studied indicating less significant fouling compared to ceramic membranes.

It can be seen from the Fig. 3 that for both the ceramic MF and UF membranes, there is a large initial variations in the permeate flux with the variations diminishing significantly, as cake layer is formed during the filtration process. This result is consistent with other study where the treatment of a primary sewage effluent using cross-flow tubular ceramic membranes with a pore size between 0.22 and 1.3 μ m demonstrated that large initial variations in the permeate flux is obtained with the variations diminishing significantly, as cake layer is formed [21]. Whereas, for the polymeric UF membrane there is no much variations in the permeate flux.

3.3. Membrane resistance and fouling models

Modelling the flux decline during filtration provides better understanding on membrane fouling and provides systematic tools for successful scale up

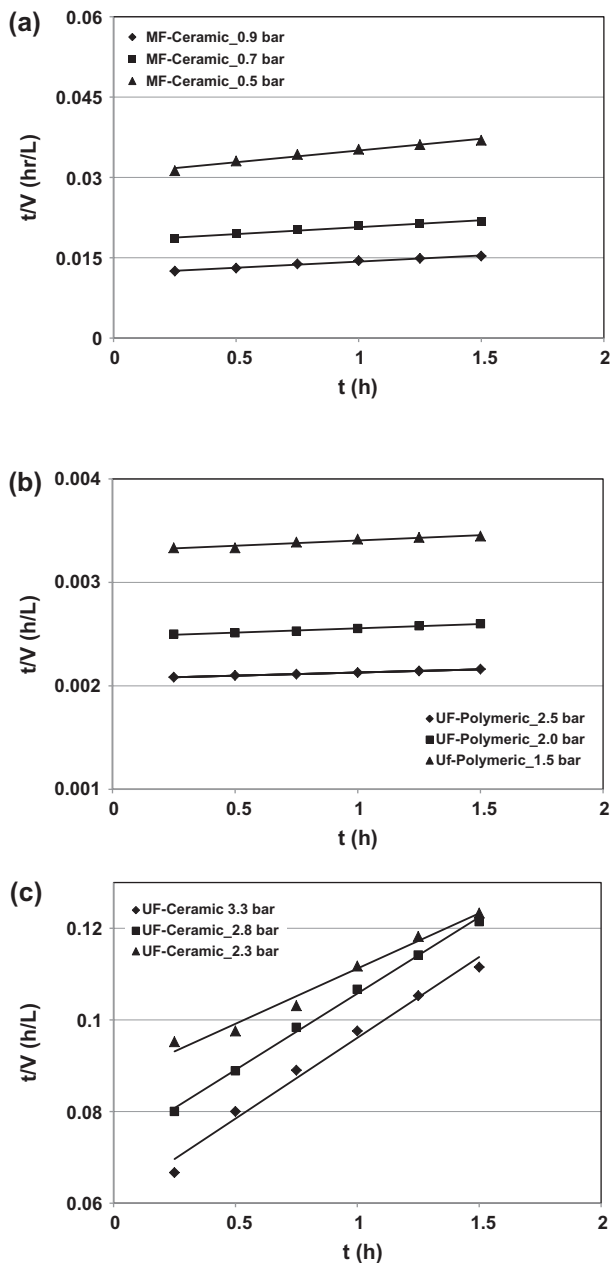


Fig. 5. Pore narrowing model fitting to the experimental data obtained in (a) ceramic MF, (b) polymeric UF and (c) ceramic UF experiments (cross flow velocity = 0.2 m/s and $T = 25^\circ\text{C}$).

or scale down of UF and MF systems. There are several models/index that could describe the performance of membrane [16,18,22,23]. They are;

- Resistance in series model
- Cake filtration model
- Pore narrowing model (progressive internal fouling)

- Combination of external and progressive internal fouling
- Complete pore blocking model
- UMFI

Brief description about these models and index is discussed below. The resistance in series model was used to evaluate resistance to the permeate flux. The cake filtration model is relevant to external fouling and combination of external and progressive internal fouling corresponds to both internal and external fouling and while pore narrowing and complete pore blocking models correspond to internal fouling. UMFI is used to quantify and assess the fouling potential of the membranes.

3.3.1. Resistance in series model

According to constant pressure theory, the permeate flux J is expressed by the resistance in-series model where ΔP is the TMP, μ the permeate viscosity and R_t the total hydraulic resistance [18].

$$J = \frac{\Delta P}{\mu R_t} \quad (2)$$

$$R_t = R_m + R_f \quad (3)$$

$$R_f = R_{if} + R_{ef} \quad (4)$$

where R_m is the hydraulic resistance of clean membrane and R_f the total (overall) fouling resistance. The external fouling resistance R_{ef} (reversible resistance) includes concentration polarisation and deposition of solids on the membrane surface. The internal fouling resistance R_{if} (irreversible resistance) is due internal fouling such as pore blocking. Table 3 summarises the resistances in every experiment conducted using all the three membranes.

The contribution to the total resistance of the fouling resistance (combined external and internal) is lower than the inherent resistance of the clean membrane in the case of the polymeric UF and same in the case of the MF membrane and higher in the case of the ceramic UF membrane. It can be seen from Table 3 that R_m is more significant for polymeric UF membrane compared to other two ceramic membranes. In the case of ceramic MF membrane, R_f is much lower than ceramic UF membrane. The highest value of R_f corresponding to the ceramic UF membrane, which is a consequence of higher amount of foulants accumulated on the surface and pores of the membrane, in particular internal component of the fouling resistance was much higher than the external

Table 5
Determination of parameter C/V_p and correlation coefficients R^2 from the pore narrowing model for UF and MF experiments

TMP bar	Initial flow rate (Q_0) (L/h)		C/V_p	Error (%)	R^2
	Model	Experimental			
<i>Ceramic MF membrane (1.4 μm)</i>					
0.9	100	103	2.3	2.912	0.989
0.7	56	60	2.6	6.666	0.969
0.5	34	38	4.4	10.526	0.975
<i>Polymeric UF membrane (25 kDa)</i>					
2.5	476	480	0.06	0.793	0.997
2.0	400	400	0.08	0	0.988
1.5	303	300	0.1	-1.01	0.935
<i>Ceramic UF membrane (1 kDa)</i>					
3.3	14.7	15	35.3	1.960	0.985
2.8	13.8	15	33	7.918	0.997
2.3	11.6	12.5	24.1	7.084	0.981

component. Also, it can be seen that the irreversible fouling resistance is higher than the reversible fouling resistance for all the three membranes. The overall fouling resistance in the three different membranes followed the sequence polymeric UF < ceramic MF < ceramic UF.

3.3.2. Cake filtration model

When wastewater is filtered through a membrane, a cake layer is being formed on the membrane surface due to the rejection of macrosolutes by the membrane. Hence, the resistance to filtration by this cake layer is assumed to increase proportionally with the volume of wastewater filtered. Thus, the total resistance to filtration, R_t could be written as:

$$R_t = R_m + \frac{\alpha C_w V_f}{A_o} \quad (5)$$

where α is the specific cake resistance per unit mass, C_w the concentration of rejected particles, V_f is the volume of filtered water and A_o is the total membrane surface area. A relationship between the filtration time, t and the volume of wastewater filtered (V_f) could be expressed as:

$$\frac{t}{V_f} = \frac{1}{Q_o} + \frac{\alpha C_w V_f}{2A_o R_m Q_o} \quad (6)$$

where Q_o is the initial Q_f of permeate. Hence, the parameters α and C_w can be evaluated by conducting

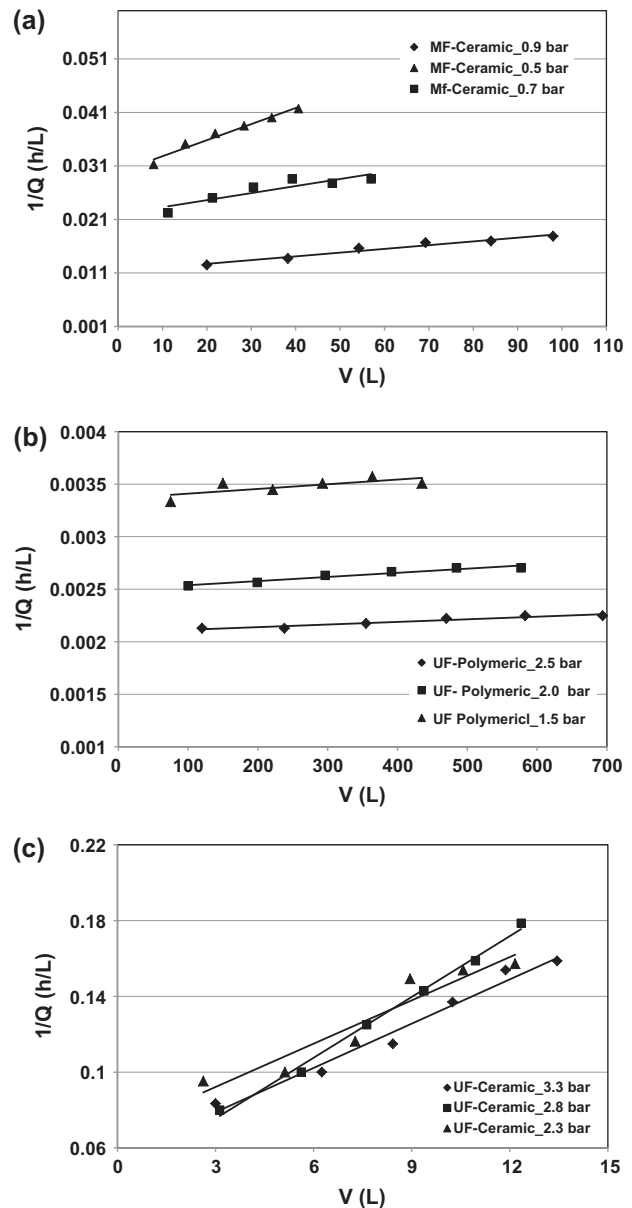


Fig. 6. Combination of external and progressive internal fouling model fitting to the experimental data obtained in (a) ceramic MF, (b) polymeric UF and (c) ceramic UF experiments (cross flow velocity = 0.2 m/s and $T = 25^\circ\text{C}$).

experiments under different operating conditions which could then be used to design membrane systems.

Fig. 4 shows the cake filtration model fitting to the experimental data obtained from three different membranes over the range of TMPs studied. While this model fits reasonably well with the data obtained for all the three membranes, the initial flux predicted by the model fits very well for both the polymeric and ceramic UF membranes. This can be seen from the Table 4 that the initial flux calculated from this model

Table 6
Combination of external and progressive internal fouling model fitting to the experimental data

TMP bar	Model input & output		Experimental value of ($\mu R_m/P A$) (h/L)	Error (%)	R^2
	$R_m \times 10^{-13}$ (m^{-1})	($\mu R_m/P A$) (h/L) (output)			
<i>Ceramic MF membrane (1.4 μm)</i>					
0.9	0.137	0.008	0.0113	29.204	0.962
0.7	0.170	0.0135	0.022	38.636	0.813
0.5	0.210	0.0233	0.0298	21.812	0.970
<i>Polymeric UF membrane (25 kDa)</i>					
2.5	1.008	0.002	0.0021	4.762	0.926
2.0	1.008	0.0025	0.0025	0	0.946
1.5	1.008	0.0033	0.0034	2.94	0.549
<i>Ceramic UF membrane (1 kDa)</i>					
3.3	1.968	0.047	0.0555	15.315	0.975
2.8	1.955	0.0554	0.0434	-27.649	0.995
2.3	1.890	0.0652	0.0693	5.916	0.911

is very close to the experimental value for both the UF membranes (Error %). This result shows that the cake filtration model is much suitable for UF membranes. Similar results were obtained by Jacob and Jaffrin [24] for UF and showed that the cake filtration model fits well for the UF membrane (15 kDa) in their study. It is interesting to note that the values of αC_w increases with decreasing TMP for polymeric UF, whereas for ceramic UF and MF membranes there is no much variations in the αC_w as TMP increases. However, the value of αC_w for ceramic UF membrane is higher than polymeric UF and ceramic MF membranes. This result is consistent with the resistance in series model, where the reversible fouling resistance of ceramic UF membrane is higher than the other two membranes.

3.3.3. Pore narrowing model

The pore narrowing model accounts for fouling that occurs in the internal structure of the membrane. In the pore narrowing model, membranes are assumed to have straight through cylindrical pores. The membrane pore radius is reduced by the uniform adsorption of macrosolutes to the internal membrane surface. The rate of change of pore volume is assumed to be proportional to the Q_f . Then, the rate of reduction of pore radius r could be expressed as:

$$2\pi N L r \left(\frac{dr}{dt} \right) = -C Q_f \quad (7)$$

where L denotes the membrane thickness, C is the dimensionless parameter characterising the fraction of solute which gets adsorbed and N is the total number

of pores on the membrane surface. Integrating the above equation with respect to time yields;

$$\frac{t}{V_f} = \frac{1}{Q_o} + \frac{Ct}{V_p} \quad (8)$$

where V_p is the initial pore volume and can be expressed as

$$V_p = \pi N r_o^2 L \quad (9)$$

where r_o is the initial pore radius. The value of C could be determined using the experimental data and would help to simulate the performance of the membrane. Fig. 5 shows the pore narrowing model fitting to the experimental data obtained from all the three membranes.

A linear regression is obtained and implies that pore narrowing model is suitable to predict the performance of the membrane filtration of wastewater. The value of initial Q_f of permeate calculated from this model is close to the experimental value for polymeric UF and ceramic MF membranes compared to ceramic UF membrane (Table 5). It is also interesting to note that the probability of adsorption (C/V_p) increases with decreasing TMP for polymeric UF and ceramic MF membranes, whereas decreases with decreasing TMP for ceramic UF membrane. The values of C/V_p of polymeric UF and ceramic MF membranes are four- and one-order of magnitude less than that of ceramic UF membrane which is consistent with the values of the irreversible resistance as shown in the Table 3. Again, this result confirms that internal fouling is more severe for ceramic UF membrane than polymeric UF and ceramic MF membranes.

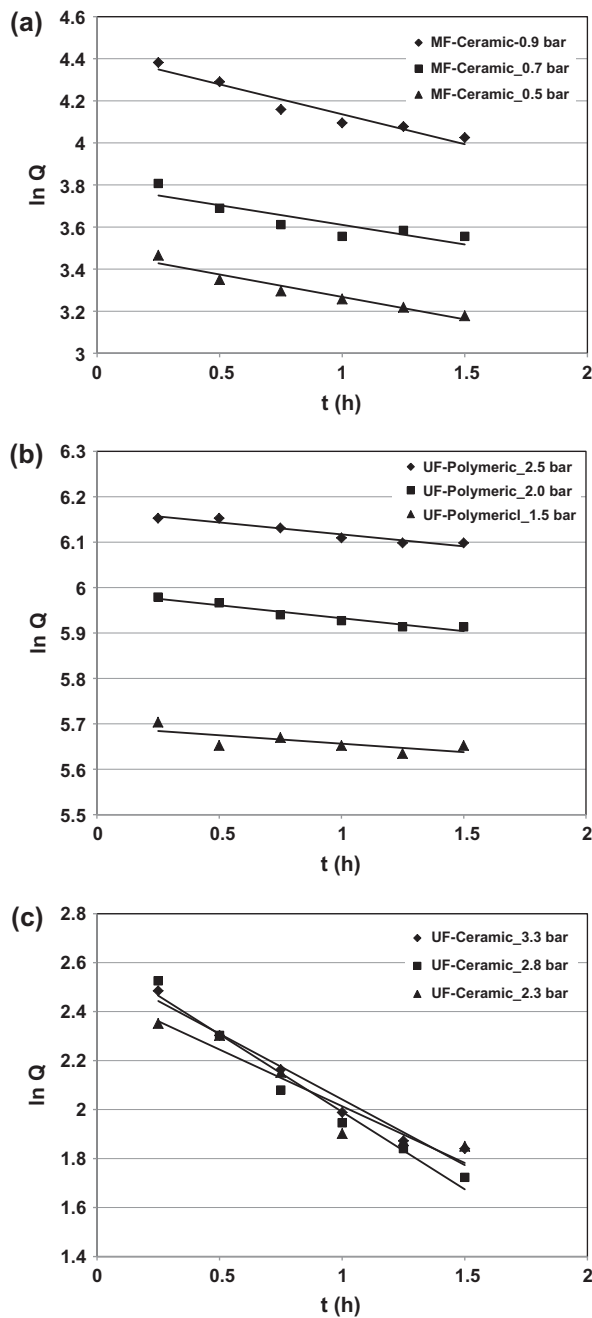


Fig. 7. Complete pore blocking model fitting to the experimental data obtained in (a) ceramic MF, (b) polymeric UF and (c) ceramic UF experiments (cross flow velocity = 0.2 m/s and $T = 25^\circ\text{C}$).

3.3.4. Combination of external and progressive internal fouling

Combination of internal and external fouling would be expected, as the wastewater contains both microsolute and rejected solutes. Thus, the cake filtration model is modified to include an increase in

the specific cake resistance due to pore narrowing. The following equation could be used in this model:

$$Q_f = \frac{\Delta P A_o}{\mu \{R_m + (\alpha C_w / A_o + 2C / V_p) V_f\}} \quad (10)$$

where ΔP is the TMP and μ is the viscosity of the permeate. According to this model, a plot of $1/Q_f$ against V_f should yield a straight line as given in the following equation;

$$\frac{1}{Q_f} = \left[\frac{\mu}{\Delta P A_o} \right] \left(\frac{\alpha C_w}{A_o} + \frac{2C}{V_p} \right) V_f + \left[\frac{\mu R_m}{\Delta P A_o} \right] \quad (11)$$

Fig. 6 shows the combination of external and progressive internal fouling model fitting to the experimental data obtained from all the three membranes. This model does not fit to the experimental data well for all the three membranes and implies that combination of external and progressive internal fouling model is not suitable to predict the performance of both the polymeric and ceramic UF and MF membranes in treating secondary effluent (Table 6).

3.3.5. Complete pore blocking model

This model considers the severe form of internal fouling because if the particle sizes are equal or close to the pore size of the membrane then the fraction of the pores are completely blocked by the particles. Thus, the surface area of the membrane A is reduced over the time as given below:

$$A = A_o - \sigma V_f \quad (12)$$

where σ is a parameter characterising the plugging potential of the suspension which is proportional to the concentration of particles in the feed solution. In this model, the flux decay is assumed to be merely due to a reduction in membrane area and not to an increase in resistance. Thus, the Q_f at a given time t can be written as:

$$Q_f = Q_o \exp(-\sigma J_o t) \quad (13)$$

where J_o is the initial permeate flux. The above equation can be rearranged as below to get a linear plot for $\ln [Q_f]$ against t :

$$\ln Q_f = \ln Q_o - \sigma J_o t \quad (14)$$

Fig. 7 shows the complete pore blocking model fitting to the experimental data for all the three membranes. This model fits to the experimental data well

Table 7

Determination of parameter σ and correlation coefficients R^2 from the complete pore blocking model for UF and MF experiments

TMP bar	Initial flow rate (Q_0) (L/h)		J_0 (L/h/m ²)	σ (m ⁻¹)	Error (%)	R^2
	Model	Experimental				
<i>Ceramic MF membrane (1.4 μm)</i>						
0.9	83.1	103	166.21	0.0017	19.316	0.932
0.7	44.5	60	89.07	0.0021	25.773	0.785
0.5	32.5	38	65.00	0.0033	14.469	0.942
<i>Polymeric UF membrane (25 kDa)</i>						
2.5	478	480	85.36	0.0006	0.418	0.922
2.0	399	400	71.30	0.0007	0.176	0.934
1.5	297	300	53.04	0.0007	1.003	0.525
<i>Ceramic UF membrane (1 kDa)</i>						
3.3	13.5	15	38.47	0.0139	10.242	0.967
2.8	13.8	15	39.36	0.0160	8.163	0.971
2.3	11.8	12.5	33.78	0.0137	5.420	0.916

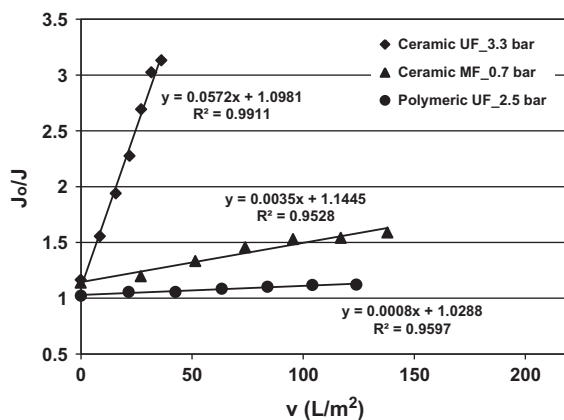


Fig. 8. J/J_0 as a function of specific permeate throughput.

for polymeric UF membrane and does not fit well with both the ceramic membranes (Table 7). Further, the plugging potential (σ) of polymeric membrane is one- and two-order of magnitude less than that of ceramic MF and ceramic UF membranes, respectively.

3.3.6. Unified Membrane Fouling index (UMFI)

UMFI is a measure of the total fouling capacity of the feedwater. The UMFI was established based on Hermia's filtration model, assuming that cake filtration was the predominant fouling mechanism but included a potential contribution from cake layer formation and pore blocking [25]. This is defined as the slope of the curve of the reciprocal of the normalised flux (J_0/J) versus accumulated specific permeate volume (v), due to the following linear relationship,

$$\frac{J_0}{J} = \left(\frac{\alpha C_w}{R_m} \right) v + 1 \quad (15)$$

where J_0 is the permeate flux at time $t=0$, J is the permeate flux through the membrane for the wastewater being tested, α is the specific resistance of the cake layer, C_w is the foulant concentration in the feed and v is the accumulated specific permeate volume (permeate volume per unit membrane area). UMFI has a unit of m²/L. As shown in the Fig. 8, UMFI for total fouling was calculated by unforced linear regression of the experimental data using Eq. 15. A greater UMFI value indicates a faster decrease in the normalised specific flux and represents the higher the membrane fouling potential.

The UMFI value in the three different membranes followed the sequence polymeric UF (0.0008 m²/L) < ceramic MF (0.0035 m²/L) < ceramic UF (0.0572 m²/L). This result is again consistent with the above results indicating ceramic UF has high fouling rate compared to other two membranes.

4. Summary and conclusions

The performance of both polymeric and ceramic membranes in filtering synthetic secondary effluent was investigated under different TMPs and the following results were obtained from this study:

- (1) Ceramic UF membrane produced high quality of water compared to polymeric UF and ceramic MF membranes, as a significant portion of the smaller colloidal particles passes through

the ceramic MF and polymeric UF membranes with larger pore sizes compared with ceramic UF membrane with smaller pore size.

- (2) There were more than 50% permeate flux decline in both the ceramic membranes and 10% permeate flux decline in the polymeric membrane across all the TMPs studied.
- (3) The overall fouling resistance in the three different membranes followed the sequence polymeric UF < ceramic MF < ceramic UF.
- (4) Out of the four fouling models used to fit the experimental flux data, the cake filtration model fitted the performance of polymeric and ceramic UF membranes more accurately compared to ceramic MF membranes.
- (5) On the other hand, the pore narrowing model fitted the performance of all the three membranes but predicted the performance of ceramic MF and polymeric UF membranes more accurately. This implies that the membrane that has the bigger pore size is more susceptible to pore narrowing.
- (6) Whereas complete pore blocking model fitted the performance of polymeric UF membrane compared to ceramic UF and MF membranes. Conversely, combination of external and progressive internal fouling model was unsatisfactory for all the three membranes.
- (7) The UMFI value in the three different membranes followed the sequence polymeric UF < ceramic MF < ceramic UF indicating a faster decrease in the normalised specific flux and higher the membrane fouling potential in ceramic UF membrane compared to polymeric UF and ceramic MF membranes.

Symbols

A_o	—	total membrane surface area (m^2)
C	—	dimensionless parameter characterising the fraction of solute which gets adsorbed
COD	—	chemical oxygen demand (mg/L)
C_w	—	concentration of rejected particles (kg/m^3)
J	—	permeate flux ($L/m^2 h$)
J_o	—	initial membrane flux ($L/m^2 h$)
L	—	membrane thickness (m)
L_p	—	pure water hydraulic permeability ($L/h m^2 bar$)
N	—	total number of pores on the membrane surface
Q_f	—	permeate flow rate (L/h)
Q_o	—	initial flow rate of permeate (L/h)
r	—	pore radius (m)
R_{ef}	—	reversible fouling resistance (m^{-1})
R_f	—	total (overall) fouling resistance (m^{-1})
R_{if}	—	irreversible fouling resistance (m^{-1})
R_m	—	hydraulic resistance of clean membrane (m^{-1})
R_t	—	total hydraulic resistance (m^{-1})
UMFI	—	unified membrane fouling index (m^2/L)
V_f	—	permeate volume (m^3)
V_p	—	initial pore volume (m^3)
α	—	specific cake resistance (m/kg)
ΔP	—	transmembrane pressure (bar)
μ	—	permeate viscosity (Pa s)
σ	—	parameter characterising the plugging potential of suspension (m^{-1})

References

- [1] S.F.E. Boerlage, M.D. Kennedy, M.R. Dickson, D.E.Y. El-Hodali, J.C. Schippers, The modified fouling index using ultrafiltration membranes (MFI-UF); characteristics, filtration mechanisms and proposed reference membrane, *J. Membr. Sci.* 197 (2002) 1–21.
- [2] R.B. Bai, H.F. Leow, Microfiltration of activated sludge wastewater—the effect of system operation parameters, *Sep. Purif. Technol.* 29 (2002) 189–198.
- [3] H. Nidal, O.O. Oluwaseun, J.M. Nick, N. Rinat, Methods employed for control of fouling in MF and UF membranes: A comprehensive review, *Sep. Sci. Technol.* 40 (2005) 1957–2005.
- [4] A.L. Ahmad, Electrophoretic membrane cleaning in dead end ultrafiltration process, Regional Symposium of Chemical Engineers UTM, 1997.
- [5] L. Fan, T. Nguyen, F.A. Roddick, J.L. Harris, Low pressure membrane filtration of secondary effluent in water reuse: Pre-treatment for fouling reduction, *J. Membr. Sci.* 32 (2008) 135–142.
- [6] S.F.E. Boerlage, M.D. Kennedy, M.P. Aniye, E.M. Abogrean, G. Galjaard, J.C. Schippers, Monitoring particulate fouling in membrane systems, *Desalination* 118 (1998) 131–142.
- [7] Y. Soffer, A. Adin, J. Gilron, Threshold flux in fouling of membranes by colloidal iron, *Desalination* 161 (2004) 207–221.
- [8] S.F.E. Boerlage, M.D. Kennedy, M.P. Aniye, E.M. Abogrean, G. Galjaard, J.C. Schippers, Monitoring particulate fouling in membrane systems, *Desalination* 118 (1998) 131–142.
- [9] S.F.E. Boerlage, M.D. Kennedy, P.A.C. Bonne, G. Galjaard, J.C. Schippers, Prediction of flux decline in membrane systems due to particulate fouling, *Desalination* 113 (1997) 231–233.
- [10] R. Sondhi, Y.S. Lin, F. Alvarez, Cross flow filtration of chromium hydroxide suspension by ceramic membranes; fouling and its minimisation by backpulsing, *J. Membr. Sci.* 174 (2000) 111–122.
- [11] E. Arkhangelsky, U. Goren, V. Gitis, Retention of organic matter by cellulose acetate membrane cleaned with hypochlorite, *Desalination* 223 (2008) 97–105.
- [12] V. Gitis, J. Gun, R.C. Haught, R.M. Clark, O. Lev, Application of nanoscale probes for the evaluation of the integrity of ultrafiltration membranes, *J. Membr. Sci.* 276 (2006) 185–192.
- [13] I.S. Chang, C.H. Lee, Membrane filtration characteristics in membrane coupled activated sludge system—the effect of physiological states of activated sludge on membrane fouling, *Desalination* 120(3) (1998) 221–233.
- [14] L. Defrance, M.Y. Jaffrin, Comparison between filtration and fixed transmembrane pressure and fixed permeate flux: Application to a membrane bioreactor used for wastewater treatment, *J. Membr. Sci.* 152 (1999) 203–210.
- [15] E. Tardieu, A. Grasmick, V. Geaugey, J. Manem, Hydrodynamic control of bioparticle deposition in a MBR applied to wastewater treatment, *J. Membr. Sci.* 147 (1998) 1–12.

- [16] H. Huang, T.A. Young, J.G. Jacangelo, Unified membrane fouling index for low pressure membrane filtration of natural waters: Principles and methodology, *Environ. Sci. Technol.* 42 (2008) 714–720.
- [17] G.T. Seo, Y. Suzuki, S. Ohgaki, Biological powdered activated carbon (BPAC) microfiltration for wastewater reclamation and reuse, *Desalination* 106 (1996) 39–45.
- [18] S. Muthukumar, D.A. Nguyen, K. Baskaran, Performance evaluation of different ultrafiltration membranes for the reclamation and reuse of secondary effluent, *Desalination* 279 (2011) 383–389.
- [19] APHA-AWWA-WEF, *Standard Methods for the Examination of Water and Wastewater*, 18th ed., American Public Health Association, Washington, DC, 1992.
- [20] C.W. Lee, S.D. Bae, S.W. Han, L.S. Kang, Application of ultrafiltration hybrid membrane processes for reuse of secondary effluent, *Desalination* 202 (2007) 239–246.
- [21] Q. Gan, S.J. Allen, Crossflow microfiltration of a primary sewage effluent-solids retention efficiency and flux enhancement, *J. Chem. Technol. Biotechnol.* 74 (1999) 693–699.
- [22] K. Konieczny, Modelling of membrane filtration of natural water for potable purposes, *Desalination* 143 (2002) 123–139.
- [23] C. Duclos-Orsello, W. Li, C. Ho, A three mechanism model to describe fouling of microfiltration membranes, *J. Membr. Sci.* 280 (2006) 856–866.
- [24] S. Jacob, M.Y. Jaffrin, Purification of brown cane sugar solutions by ultrafiltration with ceramic membranes: Investigation, *Sep. Sci. Technol.* 35(7) (2000) 989–1010.
- [25] H. Huang, T.A. Young, J.G. Jacangelo, Novel approach for the analysis of bench-scale, low pressure membrane fouling in water treatment, *J. Membr. Sci.* 334 (2009) 1–8.